

Modifying the Surface of a Rashba-Split Pb-Ag Alloy Using Tailored Metal-Organic Bonds

Benjamin Stadtmüller,^{1,2,*} Johannes Seidel,¹ Norman Haag,¹ Lisa Grad,¹ Christian Tusche,^{3,†} Gerben van Straaten,^{4,5} Markus Franke,^{4,5} Jürgen Kirschner,³ Christian Kumpf,^{4,5} Mirko Cinchetti,^{1,‡} and Martin Aeschlimann¹

¹*Department of Physics and Research Center OPTIMAS, University of Kaiserslautern, Erwin-Schroedinger-Strasse 46, 67663 Kaiserslautern, Germany*

²*Graduate School of Excellence Materials Science in Mainz, Erwin Schroedinger Straße 46, 67663 Kaiserslautern, Germany*

³*Max-Planck-Institut für Mikrostrukturphysik, 06120 Halle, Germany*

⁴*Peter Grünberg Institut (PGI-3), Forschungszentrum Jülich, 52425 Jülich, Germany*

⁵*Jülich-Aachen Research Alliance (JARA)—Fundamentals of Future Information Technology, 52425 Jülich, Germany*

(Received 23 May 2016; published 26 August 2016)

Hybridization-related modifications of the first metal layer of a metal-organic interface are difficult to access experimentally and have been largely neglected so far. Here, we study the influence of specific chemical bonds (as formed by the organic molecules CuPc and PTCDA) on a Pb-Ag surface alloy. We find that delocalized van der Waals or weak chemical π -type bonds are not strong enough to alter the alloy, while localized σ -type bonds lead to a vertical displacement of the Pb surface atoms and to changes in the alloy's surface band structure. Our results provide an exciting platform for tuning the Rashba-type spin texture of surface alloys using organic molecules.

DOI: 10.1103/PhysRevLett.117.096805

Interfaces formed between organic molecules and metal surfaces are the essential building block of a variety of novel electronic and spintronics devices. For example, hybrid interfaces control the efficiency of charge injection that limits the performance of organic light-emitting diodes [1] and organic photovoltaic cells [2]; they also determine the efficiency of spin injection across interfaces formed with ferromagnetic metals, as found in organic spin valves [3]. Along these lines, the search for better-performing, next-generation molecular-based devices has motivated extensive experimental and theoretical efforts focusing on the adsorption properties of small prototypical molecules on highly crystalline metal surfaces. These studies have provided a clear understanding of the correlation between the strength of interface hybridization and the growth of the organic molecules as well as their electronic properties, mainly described in terms of the energy level alignment at the interface [4–15].

On rather inert surfaces like gold, the molecule-substrate interaction is determined by weak van der Waals forces and the energetic positions of the molecular levels is hardly affected by the substrate [10,16–18]. On more reactive noble metal surfaces such as silver or copper, the additional chemical interactions at the interface start to influence the properties of the molecular film. This often leads to the formation of chemical bonds between the organic adsorbate and the substrate. Chemical π bonds coincide with charge transfer from the substrate into the former lowest unoccupied molecular orbital (LUMO) of the molecule [7,9,12,16,17,19,20]. On the other hand, chemical σ bonds

are more localized and lead to geometric distortions of the molecular body [8,20–22].

Crucially, in all these studies, possible modifications of the electronic and geometric properties of the first layer of substrate atoms were neglected. While this assumption might be justified for inert surfaces with weak molecule-substrate interactions, *ab initio* studies predict that it does not even hold for slightly more reactive noble metal surfaces such as Ag [20]. Recent developments in molecular spintronics also indicate that the deposition of aromatic organic molecules on the strongly reactive surfaces of ferromagnetic metals leads to a change in the local magnetic properties of the atoms hybridized with the molecule, such as exchange interaction, magnetic moments, and magnetocrystalline anisotropy [23,24]. In general, a direct experimental determination of the changes in the local structural and electronic properties of the metallic substrate remains still very challenging. It would, however, be of paramount importance, for example in the case of heavy metal-noble metal surface alloys, where the Rashba-type spin splitting of the surface states strongly depends on the vertical displacement of the heavy metal atoms.

In this Letter, we present an experimental approach to access the modification of structural and electronic properties of a Pb-Ag surface, resulting from hybridization with different adsorbate molecules. We discuss two cases exhibiting fundamentally different behavior caused by the functional groups of the molecules that form preferentially π - or σ -type chemical bonds. Because of the intrinsic nature of the Pb-Ag surface, the Pb atoms can be used as tracers,

whose relative position with respect to the Ag atoms can be determined experimentally with high accuracy ($< 0.04 \text{ \AA}$) by using the normal incidence x-ray standing waves (NIXSW) technique. The chemical sensitivity of this technique allows us to distinguish the adsorption height of the metallic tracer atoms from the host atoms and to measure the molecule-substrate bonding distance. A detailed analysis of the NIXSW data is outside the scope of this Letter and will be published elsewhere [25]. To access the modifications in the electronic surface band structure of the metal surface, we employ the uniqueness of momentum microscopy [26,27]. This experimental tool for photoelectron spectroscopy provides two-dimensional momentum space emission patterns in constant binding energy (CBE) cuts through the band structure in the entire accessible momentum range. For molecular emission signals, the photoemission distribution of these CBE maps can be used to assign spectroscopic photoemission features to the emitting molecular orbital [28].

The Pb-Ag surface alloy formed on a Ag(111) surface is part of a wide class of long-range ordered surface alloys, which have attracted great attention in the field of spintronics due to a spiral spin texture of hybrid surface states caused by the Rashba-Bychkov effect [29–34]. For the pristine Pb_1Ag_2 surface alloy on Ag(111), each third silver atom in the first silver layer is replaced by Pb leading to the formation of a long-range ordered surface alloy with the well-known $(\sqrt{3} \times \sqrt{3})R30^\circ$ superstructure [29,30]. Vertically, the Pb_1Ag_2 alloy layer shows a significant buckling and a vertical displacement of the Pb atoms due to their significantly larger size compared to Ag [30], as illustrated in Fig. 1(a). Thereby, the vertical displacement of the Pb atoms is the decisive parameter that determines the spin texture of the Rasha-type spin splitting of the surface states of the Pb-Ag alloy [30,31,35,36]. In agreement with a previous LEED-IV study [30], all Pb atoms are located $0.42 \pm 0.02 \text{ \AA}$ above the plane of the Ag surface atoms, which are at the vertical position of the Ag lattice planes of the bulk crystal.

As organic adsorbates, we have chosen the two prototypical organic molecules copper-II-phthalocyanine (CuPc) and 3,4,9,10-perylene-tetracarboxylic-dianhydride (PTCDA).

They are of particular interest since they interact differently with metallic surfaces. While CuPc interacts only via its delocalized π system with noble metal surfaces [4,9,16,19,37], PTCDA reveals a π bond and additional local σ -like bonds formed between the oxygen atoms of the anhydride end groups and metallic surface atoms [4,20,38]. Hence, interfaces between CuPc and PTCDA, respectively, and the Pb_1Ag_2 surface alloy are ideal models to reveal how geometric, electron, and spin-specific properties of metal surfaces are altered by π and σ bonding between molecules and surfaces.

Panels (b) and (c) of Fig. 1 show the vertical adsorption geometry of the monolayer CuPc and PTCDA films, respectively, deposited on the Pb_1Ag_2 surface as determined by NIXSW. Within the experimental uncertainty, CuPc does not influence the vertical displacement of the Pb tracer atoms and the Ag surface atoms. The molecular body is found in an almost flat adsorption configuration at an adsorption height of $3.76 \pm 0.02 \text{ \AA}$. This adsorption height is significantly larger than on the pristine Ag(111) surface ($3.08 \pm 0.02 \text{ \AA}$) [19] and even exceeds the van der Waals bonding distance of the molecule and the silver surface. This indicates that CuPc does not interact with the Ag surface atoms. In contrast, the bonding distance between the molecular body and the Pb atoms is smaller than the corresponding van der Waals distance, indicating a nonvanishing delocalized π bond between CuPc and the Pb atoms.

For the adsorption of PTCDA, our results are clearly different. We find an additional vertical displacement of all Pb atoms of $0.08 \pm 0.02 \text{ \AA}$ which is uniform for the entire molecular film. At first glance, this is surprising since we find two distinct adsorption sites *A* and *B* for PTCDA with two clearly different adoption heights. The latter finding is further supported by high-resolution core level spectroscopy that proves the existence of two (chemically) inequivalent molecular contributions to the $\text{C}1s$ core level yield [25]. For adsorption site *A*, the PTCDA backbone is found at a smaller adsorption height than CuPc indicating a stronger π bonding to the surface, for the other site *B*, it is at almost the same adsorption height pointing to a similar

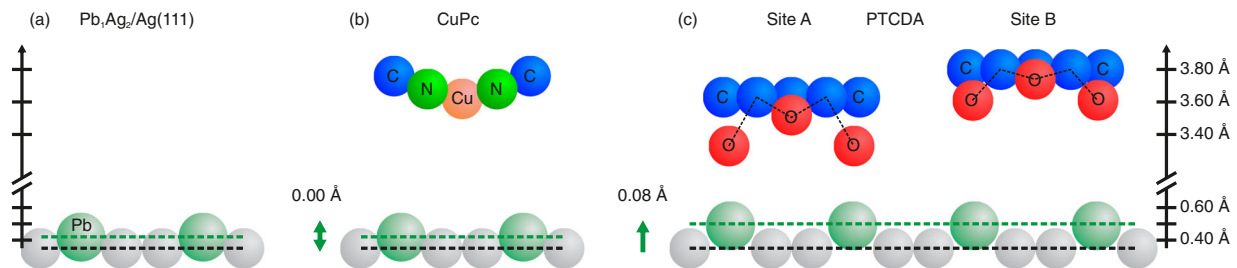


FIG. 1. Model of the vertical adsorption geometry of the buckling of the pristine Pb-Ag surface alloy (a), as well as of CuPc (b) and PTCDA (c) adsorption on the Pb-Ag surface alloy as determined by NIXSW. For CuPc only one or two atoms are shown for each species while both structurally inequivalent PTCDA molecules (*A*, *B*) are shown in a side view on its shorter side.

π -bonding strength across the interface. Most noticeable, all oxygen species of the functional anhydride end groups are located below the molecular plane for both PTCDA adsorption sites pointing to an M -like distortion of PTCDA. This adsorption configuration is well known for more reactive noble metal surfaces on which PTCDA forms local σ bonds to the metal surface via its oxygen end groups [20]. In analogy, the down bending of the oxygen atoms is clear proof for the formation of local σ bonds between PTCDA and the atoms of the surface alloy. Since the vertical distance between the oxygen atoms of PTCDA and the Ag surface atoms is significantly larger than the typical O-Ag bonding distances, we must conclude that PTCDA bonds locally to Pb atoms of the surface alloy. These σ bonds are hence responsible for the additional vertical displacement of the Pb atoms. These experimental results confirm the theoretical predictions by Bauer *et al.* [20], who proposed a vertical relaxation of surface atoms due to the formation of local bonds across metal-organic interfaces.

After the geometrical modifications of the surface, we now discuss the changes in the band structure of the Pb_1Ag_2 alloy induced by CuPc and PTCDA as detected by momentum microscopy. The right part of Fig. 2(a) shows the CBE map of the bare surface alloy recorded at the Fermi energy, and is compared to the CBE map of the clean Ag(111) surface on the left side. The circular band in the center of the surface Brillouin zone is magnified in the inset of Fig. 2(a). This Pb-Ag hybrid surface state shows a Rashba-type spin splitting into two concentric circles [29,32], that results from the strong spin-orbit coupling of the Pb atoms. In addition, a second Pb-Ag hybrid surface state evolves at the $-\bar{M}$ point of the Ag(111) surface Brillouin zone having a band gap at E_F [29,32].

These Pb-Ag bands can be used as fingerprints of the influence of the molecule-substrate interaction on the electronic properties of the first metal layer. In our experimental geometry, we take advantage of the gracing angle of incidence of the vacuum ultraviolet radiation (65° with respect to the sample normal) that leads to a strong asymmetry in the molecular emission pattern due to the linear dichroism in the angular distribution [39]. Hence, in the forward direction of the incoming light, all CBE maps of molecular orbitals exhibit much stronger molecular features (positive momenta, see Supplemental Material [40]) while almost no signal from the molecules can be detected in backward emission directions [negative momenta, left side of our CBE maps in Figs. 2(b)–2(d)]. As we are most interested in the metallic band structure underneath the molecular film, we will only use that half of the CBE map recorded for backward emission for discussing adsorption-induced changes of the electronic properties of the first metal layer. The right parts of the CBE maps in Figs. 2(b)–2(d) are replaced by CBE maps of appropriate reference systems, as discussed in the following.

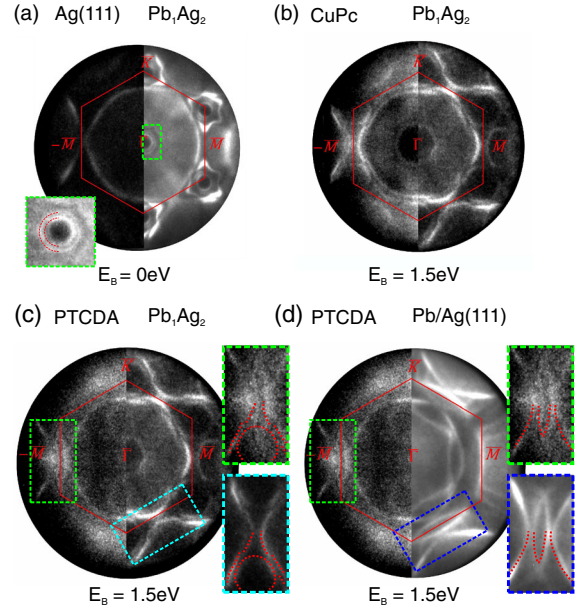


FIG. 2. Constant binding energy maps of the Fermi surface of the pristine Pb-Ag surface alloy (a), of the HOMO regions of CuPc (b) and PTCDA (c),(d). The left halves of (b), (c), and (d) show the emission of the substrate bands underneath the molecular film; the right halves show the band structure of the pristine Pb-Ag surface alloy (b), (c) and of a Pb monolayer film on Ag(111) (d), respectively. The insets of panels (c) and (d) show magnified momentum space regions around the symmetry equivalent $-\bar{M}$ points highlighted with identical color in the corresponding CBE maps. The momentum space curvature of both reference systems is modeled by B -spline functions (red dotted lines in lower insets) that are superimposed onto the momentum space curvature of the PTCDA covered Pb-Ag surface alloy (red dotted lines, upper insets).

We start with the discussion of CuPc/ Pb_1Ag_2 and the CBE maps at $E_B = 1.5$ eV in Fig. 2(b). All features of the pristine Pb_1Ag_2 alloy band structure [right part of the CBE map in Fig. 2(b)] are also clearly visible for the CuPc covered surface [left part of the CBE map in Fig. 2(b)]. A quantitative analysis of the dispersion of the Pb-Ag Rashba state reveals no energy shift caused by CuPc. We thus conclude that the band structure of Pb_1Ag_2 is not changed by the adsorption of CuPc, in agreement with our NIXSW results revealing no additional vertical displacement of the Pb atoms.

The situation is significantly different in the case of PTCDA adsorption. This is evident from the left part of the CBE shown in Fig. 2(c) which shows the surface band structure underneath the molecular film at $E_B = 1.5$ eV. Here, the Pb-Ag surface state in the center of the Brillouin zone vanishes completely, and the Pb-Ag hybrid bands close to the $-\bar{M}$ points of the Ag(111) Brillouin zone are replaced by new emission features. This becomes clear when considering the momentum space regions around the $-\bar{M}$ points which are enlarged in the insets of Fig. 2(c). The

band structure of the surface alloy (lower inset) is replaced by an elliptically shaped band at the $-\bar{M}$ point which is surrounded by two bands with a hyperbolic curvature in momentum space (upper inset). When comparing our results to CBE maps of different Pb-Ag metallic surfaces, we find the best agreement (see Supplemental Material [40]) with the band structure of a pristine Pb monolayer film adsorbed on Ag(111) [41] shown in the right part of Fig. 2(d). The corresponding enlarged momentum space region close to the $-\bar{M}$ point is shown in the inset of Fig. 2(d). For comparison, the momentum space curvature of the Pb monolayer film is modeled by B -spline functions (dotted red lines) and superimposed onto the momentum space region of the PTCDA covered surface.

The correspondence between the momentum space signatures of the PTCDA/Pb₁Ag₂ interface and the Pb-monolayer film on Ag(111) indicates that the adsorption of PTCDA causes a strong modification of the electronic properties of the Pb₁Ag₂ surface, which effectively results in a change of the surface band structure from “Pb-Ag alloy-like” to “Pb-Ag monolayer-like.” This transition occurs uniformly for the entire molecular film since all photoemission signatures of the bands of the Pb-Ag alloy are replaced by new emission features of Pb-Ag monolayer-like bands, similar to the homogeneous vertical displacement of all Pb atoms of the surface alloy.

Hence, the following picture emerges for the modification of the geometric and electronic properties of the Pb₁Ag₂ surface alloy: For the adsorption of CuPc, we find clear indications for a delocalized π bond between the molecule and the surface which leaves the vertical displacement of Pb atoms and the Pb-Ag band structure unaffected. In contrast, the formation of π bonds of different strength and additional σ bonds between two structurally different PTCDA molecules and the Pb-Ag surface results in a significant vertical displacement of all Pb atoms and in a band structure transition from Pb-Ag alloy-like to Pb-Ag monolayer-like. Because of the existence of two different types of bonding (π and σ bonding), it is not unambiguously clear which of them is responsible for the modifications of the substrate properties.

To investigate this aspect, we study the charge reorganization across these different interfaces using momentum microscopy. This will allow us to gain insight into the strength of the delocalized π bonds formed at the CuPc/Pb₁Ag₂ and PTCDA/Pb₁Ag₂ interface. Figure 3 shows the total ultraviolet photoemission (UPS) yield extracted from the momentum microscopy data of both interfaces. For CuPc, only one molecular feature is visible in the valence band range at $E_B = 1.5$ eV. According to the CBE map recorded at this binding energy and shown in the left column of Fig. 3, this state can be assigned to the highest occupied molecular orbital (HOMO) of CuPc and is found at almost the same energy position as for CuPc/Ag(111) [19]. More importantly, no second

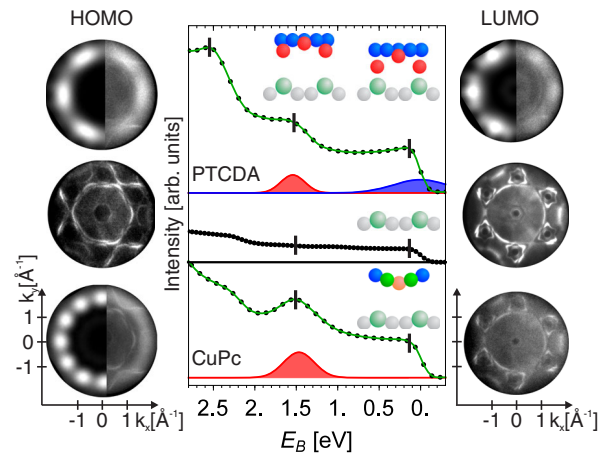


FIG. 3. UPS spectra of a monolayer film CuPc (lower spectrum) and PTCDA (upper spectrum) adsorbed on a Pb-Ag surface alloy. As reference, the UPS spectrum of the pristine Pb-Ag is shown in the middle. The left column shows constant binding energy maps of the momentum resolved photoemission intensity record at the HOMO binding energy ($E_B = 1.5$ eV); the right column at the Fermi energy. In all CBE maps containing molecular features, the left half of the CBE maps show the theoretical calculations of the momentum space distribution of the corresponding molecular orbitals calculated for free molecules; the right half shows the experimental data. All data are obtained at room temperature using a momentum microscope and illumination by a helium discharge light source ($\hbar\omega = 21.22$ eV).

molecular signal is found right at the Fermi energy. This indicates a vanishing charge reorganization between CuPc and the surface alloy, and a negligible chemical interaction across the interface. Hence, the π bonding between CuPc and the surface alloy is driven purely by van der Waals-like forces and physisorption.

The UPS data for PTCDA are more complex and reveal three distinct molecular features at $E_B = 2.5$, 1.5, and 0.1 eV. By inspection of the corresponding CBE maps, the first two signals are assigned to the HOMO levels of both structurally inequivalent PTCDA molecules at sites B and A, in agreement with a previous study of PTCDA on Bi-Ag surface alloy [42]. However, most remarkable is that a molecular contribution close to the Fermi level is visible in the UPS data for PTCDA/Pb₁Ag₂. In analogy to the adsorption of PTCDA on more reactive noble metal surfaces, we assign this state to the LUMO of PTCDA, which becomes at least partially populated due to charge reorganization across the metal-organic interface [9,12,16]. Based on the significantly lower adsorption height of PTCDA at site A, we conclude that charge transfer into the π -type LUMO only occurs for PTCDA molecules at that site, but not for those at site B. Therefore, only this type of PTCDA molecule forms a chemical π bond with the surface alloy. The PTCDA molecule at adsorption site B forms a van der Waals-like π bond, similar to the one for CuPc/Pb₁Ag₂.

Based on our experimental findings, we have substantial evidence that the band structure transition and the vertical displacement of Pb atoms is only the result of local σ bonds between the oxygen atoms of PTCDA and the Pb atoms of the first surface layer. (i) The band structure transition occurs uniformly for the molecular film, in analogy to the homogeneous vertical displacement of the Pb atoms and the down bending of the oxygen atoms observed for both structurally inequivalent PTCDA species on site *A* and *B*. In particular, this homogeneity of substrate modifications excludes the chemical π bond between PTCDA and the surface Pb_1Ag_2 alloy as a driving mechanism as it only occurs for one PTCDA species (site *A*). Instead, they are the result of σ bonds between the oxygen atoms of PTCDA and the Pb atoms of the modified Ag(111) surface. (ii) Any change of the vertical position of the alloy atoms Pb should first of all result in a reduction or an enhancement of the spin splitting of the Pb-Ag hybrid state and not in the formation of new bands [30,31,35,36]. Only additional σ bonds can severely change the local chemical environment of the heavy metal atoms leading to the formation of novel bands. In our case, the Pb atoms are surrounded by Ag atoms in the surface plane as well as below the surface plane. Upon adsorption of PTCDA, the formation of local (σ -like) O-Pb bonds induces an additional interaction partner above the surface. This leads to a significantly different chemical environment in the surface plane and perpendicular to the surface plane, which in turn changes the vertical displacement of the Pb atoms and leads to a band structure transition from Pb-Ag alloy-like to Pb-Ag monolayer-like.

In conclusion, we were able to reveal a clear connection between the bonding mechanism and strength across metal-organic hybrid interfaces and the resulting modifications of the geometric and electronic properties of the metallic substrate. For weak van der Waals-like interactions or even delocalized (weak) chemical π bonds between the organic adsorbate and the substrate surface, the vertical displacement of surface atoms of the first metal layer and the corresponding band structure remains unchanged. In contrast, local, σ -like bonds between functional groups of the adsorbate and the Pb atoms of the surface alloy can strongly modify the geometric and electronic properties of the substrate surface. Our findings demonstrate the potential of organic molecules to functionalize surfaces by the appropriate choice of functional groups forming local interface bonds. In particular, for heavy metal-noble metal surface alloys, a site specific interaction of functionalized molecular groups could be the key to enhance, reduce, or suppress the Rashba-type spin splitting of surface states. This approach can open a new route to functionalize surface structures with distinct spin textures by organic molecules.

The experimental work carried out in the University of Kaiserslautern was funded by the SFB/TRR 173

Spin + X: spin in its collective environment (Project B05) from the DFG. B. S. thankfully acknowledges financial support from the Graduate School of Excellence MAINZ (Excellence Initiative DFG/GSC 266). The authors thank Pardeep K. Thakur and Tien-Lin Lee for their support at the beamline I09 of Diamond Light Source.

*bstadtmueller@physik.uni-kl.de

†Present address: Peter Grünberg Institut (PGI-6), Forschungszentrum Jülich, 52425 Jülich, Germany.

‡cinchett@rhrk.uni-kl.de

- [1] J. Kido, M. Kimura, and K. Nagai, *Science* **267**, 1332 (1995).
- [2] D. Wöhrle and D. Meissner, *Adv. Mater.* **3**, 129 (1991).
- [3] V. A. Dediu, L. E. Hueso, I. Bergenti, and C. Taliani, *Nat. Mater.* **8**, 707 (2009).
- [4] A. Hauschild, K. Karki, B. C. C. Cowie, M. Rohlfing, F. S. Tautz, and M. Sokolowski, *Phys. Rev. Lett.* **94**, 036106 (2005).
- [5] G. Heimel *et al.*, *Nat. Chem.* **5**, 187 (2013).
- [6] C. Stadler, S. Hansen, I. Kröger, C. Kumpf, and E. Umbach, *Nat. Phys.* **5**, 153 (2009).
- [7] W. Liu, F. Maaß, M. Willenbockel, C. Bronner, M. Schulze, S. Soubatch, F. S. Tautz, P. Tegeder, and A. Tkatchenko, *Phys. Rev. Lett.* **115**, 036104 (2015).
- [8] S. Duhm *et al.*, *ACS Appl. Mater. Interfaces* **5**, 9377 (2013).
- [9] M. Willenbockel, D. Lüftner, B. Stadtmüller, G. Koller, C. Kumpf, S. Soubatch, P. Puschnig, M. G. Ramsey, and F. S. Tautz, *Phys. Chem. Chem. Phys.* **17**, 1530 (2015).
- [10] D. A. Egger, Z.-F. Liu, J. B. Neaton, and L. Kronik, *Nano Lett.* **15**, 2448 (2015).
- [11] S. Berkebile *et al.*, *Phys. Chem. Chem. Phys.* **13**, 3604 (2011).
- [12] J. Ziroff, F. Forster, A. Schöll, P. Puschnig, and F. Reinert, *Phys. Rev. Lett.* **104**, 233004 (2010).
- [13] Y. L. Huang, E. Wruss, D. A. Egger, S. Kera, N. Ueno, W. A. Saidi, T. Bucko, A. T. S. Wee, and E. Zojer, *Molecules* **19**, 2969 (2014).
- [14] M. Gottfried, *Surf. Sci. Rep.* **70**, 259 (2015).
- [15] C. H. Schwalb, S. Sachs, M. Marks, A. Schöll, F. Reinert, E. Umbach, and U. Höfer, *Phys. Rev. Lett.* **101**, 146801 (2008).
- [16] S. Duhm, A. Gerlach, I. Salzmann, B. Braeker, R. Johnson, F. Schreiber, and N. Koch, *Org. Electron.* **9**, 111 (2008).
- [17] B. Stadtmüller, I. Kröger, F. Reinert, and C. Kumpf, *Phys. Rev. B* **83**, 085416 (2011).
- [18] D. Lüftner, M. Milko, S. Huppmann, M. Scholz, N. Ngyuen, M. Wießner, A. Schöll, F. Reinert, and P. Puschnig, *J. Electron Spectrosc. Relat. Phenom.* **195**, 293 (2014).
- [19] I. Kröger *et al.*, *New J. Phys.* **12**, 083038 (2010).
- [20] O. Bauer, G. Mercurio, M. Willenbockel, W. Reckien, C. H. Schmitz, B. Fiedler, S. Soubatch, T. Bredow, F. S. Tautz, and M. Sokolowski, *Phys. Rev. B* **86**, 235431 (2012).
- [21] S. K. M. Henze, O. Bauer, T.-L. Lee, M. Sokolowski, and F. S. Tautz, *Surf. Sci.* **601**, 1566 (2007).
- [22] C. Bürker, N. Ferri, A. Tkatchenko, A. Gerlach, J. Niederhausen, T. Hosokai, S. Duhm, J. Zegenhagen, N. Koch, and F. Schreiber, *Phys. Rev. B* **87**, 165443 (2013).

- [23] R. Friedrich, V. Caciuc, N. S. Kiselev, N. Atodiresei, and S. Blügel, *Phys. Rev. B* **91**, 115432 (2015).
- [24] N. Atodiresei, J. Brede, P. Lazić, V. Caciuc, G. Hoffmann, R. Wiesendanger, and S. Blügel, *Phys. Rev. Lett.* **105**, 066601 (2010).
- [25] B. Stadtmüller, N. Haag, J. Seidel, G. van Straaten, M. Franke, C. Kumpf, M. Cinchetti, and M. Aeschlimann (to be published).
- [26] B. Krömker, M. Escher, D. Funnemann, D. Hartung, H. Engelhard, and J. Kirschner, *Rev. Sci. Instrum.* **79**, 053702 (2008).
- [27] Special issue: LEEM-PEEM 9 [C. Tusche, A. Krasnyuk, and J. Kirschner, *Ultramicroscopy* **159**, 520 (2015)].
- [28] P. Puschnig, S. Berkebile, A. J. Fleming, G. Koller, K. Emtsev, T. Seyller, J. D. Riley, C. Ambrosch-Draxl, F. P. Netzer, and M. G. Ramsey, *Science* **326**, 702 (2009).
- [29] D. Pacilé, C. R. Ast, M. Papagno, C. Da Silva, L. Moreschini, M. Falub, A. P. Seitsonen, and M. Grioni, *Phys. Rev. B* **73**, 245429 (2006).
- [30] I. Gierz, B. Stadtmüller, J. Vuorinen, M. Lindroos, F. Meier, J. H. Dil, K. Kern, and C. R. Ast, *Phys. Rev. B* **81**, 245430 (2010).
- [31] H. Bentmann, F. Forster, G. Bihlmayer, E. V. Chulkov, L. Moreschini, M. Grioni, and F. Reinert, *Europhys. Lett.* **87**, 37003 (2009).
- [32] C. R. Ast, J. Henk, A. Ernst, L. Moreschini, M. C. Falub, D. Pacilé, P. Bruno, K. Kern, and M. Grioni, *Phys. Rev. Lett.* **98**, 186807 (2007).
- [33] L. El-Kareh, G. Bihlmayer, A. Buchter, H. Bentmann, S. Blügel, F. Reinert, and M. Bode, *New J. Phys.* **16**, 045017 (2014).
- [34] D. Guan, M. Bianchi, S. Bao, E. Perkins, F. Meier, J. H. Dil, J. Osterwalder, and P. Hofmann, *Phys. Rev. B* **83**, 155451 (2011).
- [35] H. Bentmann and F. Reinert, *New J. Phys.* **15**, 115011 (2013).
- [36] L. Moreschini, A. Bendounan, H. Bentmann, M. Assig, K. Kern, F. Reinert, J. Henk, C. R. Ast, and M. Grioni, *Phys. Rev. B* **80**, 035438 (2009).
- [37] L. Kilian *et al.*, *Phys. Rev. Lett.* **100**, 136103 (2008).
- [38] M. Rohlfing, R. Temirov, and F. S. Tautz, *Phys. Rev. B* **76**, 115421 (2007).
- [39] N. A. Cherepkov and G. Schönhense, *Europhys. Lett.* **24**, 79 (1993).
- [40] See Supplemental Material at <http://link.aps.org/supplemental/10.1103/PhysRevLett.117.096805> for details on the treatment of the momentum microscopy data in Fig. 2, experimental data on the dispersion of the Pb-Ag surface state for the bare Pb-Ag alloy and the CuPc covered surface, and momentum microscopy data for additional relevant reference systems containing Pb and Ag.
- [41] C. R. Ast, D. Pacilé, M. Papagno, T. Gloor, F. Mila, S. Fedrigo, G. Wittich, K. Kern, H. Brune, and M. Grioni, *Phys. Rev. B* **73**, 245428 (2006).
- [42] M. Cottin, J. Lobo-Checa, J. Schaffert, C. Bobisch, R. Möller, J. Ortega, and A. Walter, *New J. Phys.* **16**, 045002 (2004).